UHPC Connections for Prefabricated Bridge Elements: Embedment and Splice of Reinforcement

Jiqiu Yuan[1] and Benjamin Graybeal[2]

[1] Ph.D., P.E., PSI, Inc., Turner-Fairbank Highway Research Center
[2] Ph.D., P.E., FHWA, Turner-Fairbank Highway Research Center
6300 Georgetown Pike, McLean, VA, 22101, US

The use of prefabricated bridge elements necessitates the use of field-cast connections between these bridge elements. One promising connection concept entails the use of ultra-high performance concrete (UHPC) as the field-cast grout material to fill and complete the connection. The reinforcement detailing requirements were investigated and are reported through this work. The bond behavior of reinforcing steel in UHPC is investigated by conducting direct tension pullout tests. The effect of design parameters, including the embedment length, concrete cover, bar spacing, bar size, bar type, concrete strength, and fiber content on bond strength were assessed. It was found that the bond behavior of reinforcing steel in UHPC is different from that in traditional concrete in many respects. The advanced material properties of UHPC allow for significant reduction on the embedment length, leading to cleaner connection designs and simpler construction. Guidance on the embedment of reinforcing bars into UHPC is provided.

Keywords: Ultra-High Performance Concrete, UHPC, Connection, Prefabricated Bridge Element, Bond, Embedment Length

INTRODUCTION

The use of prefabricated bridge elements necessitates the use of field-cast connections between these bridge elements. One promising connection concept entails the use of ultra-high performance concrete (UHPC) as the field-cast grout material to fill and complete the connection. UHPC is a relatively new class of cementitious composite materials. These concretes tend to contain high cementitious materials contents and very low water-to-cementitious materials ratio, and to include high volume of steel fiber reinforcement. The discrete steel fiber reinforcement included in UHPC allows the concrete to maintain tensile capacity beyond cracking of the cementitious matrix. UHPC has been defined as follows:

UHPC is a cementitious composite material composed of an optimized gradation of granular constituents, a water-to-cementitious materials ratio less than 0.25, and a high percentage of discontinuous internal fiber reinforcement. The mechanical properties of UHPC include compressive strength greater than 21.7 ksi (150 MPa) and sustained post-cracking tensile strength greater than 0.72 ksi (5 MPa). UHPC has a discontinuous pore structure that reduces liquid ingress, significantly enhancing durability compared to conventional concrete.[1]

Typical field-cast UHPC material properties are presented in Table 1, which represents average values for a number of test parameters relevant to the use of UHPC as obtained from

Table 1. Typical field-cast UHPC material properties.

Material Characteristic	Average Result
Density	2,480 kg/m^3 (155 lb/ft^3)
Compressive Strength (ASTM C39; 28-day strength)	126 MPa (18.3 ksi)
Modulus of Elasticity (ASTM C469; 28-day modulus)	42.7 GPa (6200 ksi)
Split Cylinder Cracking Strength (ASTM C496)	9.0 MPa (1.3 ksi)
Prism Flexure Cracking Strength (ASTM C1018; 305-mm (12-in.) span)	9.0 MPa (1.3 ksi)
Mortar Briquette Cracking Strength (AASHTO T132)	6.2 MPa (0.9 ksi)
Direct Tension Cracking Strength (Axial tensile load)	5.5–6.9 MPa (0.8–1.0 ksi)
Prism Flexural Tensile Toughness (ASTM C1018; 305-mm (12-in.) span)	I_{30} = 48
Long-Term Creep Coefficient (ASTM C512; 77 MPa (11.2 ksi) load)	0.78
Long-Term Shrinkage (ASTM C157; initial reading after set)	555 microstrain
Total Shrinkage (Embedded vibrating wire gage)	790 microstrain
Coefficient of Thermal Expansion (AASHTO TP60–00)	14.7 x10^{-6} mm/mm/ºC (8.2 x10^{-6} in./in./ºF)
Chloride Ion Penetrability (ASTM C1202; 28-day test)	360 coulombs
Chloride Ion Permeability (AASHTO T259; 12.7-mm (0.5-in.) depth)	< 0.06 kg/m^3 (< 0.10 lb/yd^3)
Scaling Resistance (ASTM C672)	No Scaling
Abrasion Resistance (ASTM C944 2x weight; ground surface)	0.73 grams lost (0.026 oz. lost)
Freeze-Thaw Resistance (ASTM C666A; 600 cycles)	RDM = 112%
Alkali-Silica Reaction (ASTM C1260; tested for 28 days)	Innocuous

independent testing of a commercially available product[2]. It should be noted that the UHPC investigated in that study was designed for precast applications with accelerated curing and thus exhibited a reduced compressive strength under field casting and curing applications as compared to some currently available UHPC products.

The advanced mechanical properties of the UHPC materials have enabled possibilities for more simple and robust designs in structural applications. One of the major efforts of using UHPC in infrastructure industry is to construct UHPC connections between prefabricated bridge elements. A few specific connection details, such as those discussed in *Behavior of Field-Cast Ultra-High Performance Concrete Bridge Deck Connections Under Cyclic and Static Structural Loading* and *Development of a Field-Cast Ultra-High Performance Concrete Composite Connection Detail for Precast Concrete Bridge Decks*, have been rigorously tested at service and ultimate performance limits.[3,4] The box beam connection study by Yuan and Graybeal[5,6] compared the performance of the innovative UHPC connections with the traditional post-tensioned conventional grout connections and concluded that the UHPC connections can be expected to be comparable with well-constructed monolithic concrete decks. An example of the partial-depth UHPC shear key design from Yuan and Graybeal's study is presented in Figure 1.

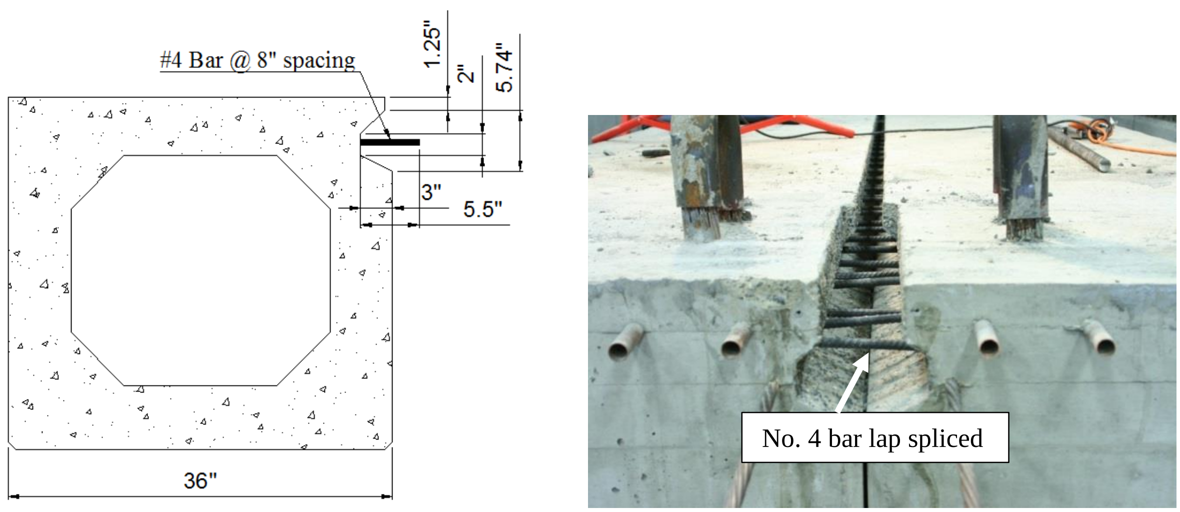

Figure 1. An example of the partial-depth UHPC shear key design. Note: 1 in. = 25.4mm

A handful of State DOTs have deployed UHPC components within their infrastructure, and many more are actively considering the use of UHPC. As late 2013, 34 bridges in the United States have been constructed using field-cast UHPC connections.[7]

As a relatively new material, limited research has been conducted on the reinforcement development in UHPC and most research[8-11] only investigated a few factors with very limited tests. This paper is part of the study conducted at the FHWA Turner-Fairbank Highway Research Center as an effort to characterize the bond behavior of reinforcing steel in UHPC materials.

EXPERIMENTAL SETUP

PULLOUT TESTS SETUP

The bond of reinforcement in UHPC is investigated by conducting pullout tests. With the recognition that the embedment length can be significantly reduced for reinforcing steel in UHPC, a novel pullout test specimen design was developed in the study. The pullout test specimens were UHPC strips cast on top of precast slabs, with the testing bar embedded in the middle of the strip, as shown in Figure 2. The UHPC strips were held down to the precast concrete slab by the pre-embedded No. 8 bars in the slab. The pullout tests were then conducted using the fixture shown in Figure 3. When a pullout force is applied, the fixture reacts against the precast slab. With such a setup, the reinforcing bars being tested as well as the concrete around the steel bar and the extended No. 8 bars from the slab are all placed in tension. The UHPC surrounding these bars transfers the loads between them. This test setup simulates structural configurations wherein non-contact lap spliced reinforcement and surronding concrete are loaded in tension. During the pullout tests, the bar displacement was measured at the loaded end, approximately two inches (51 mm) above the top surface of the UHPC strip. Both the load and loaded end displacement were recorded during the tests. More details about testing setup can be found in the associated research report and paper. [12,13]

In Figure **2** and Figure **3**, notations were assigned to represent dimension parameters, including c_{so} for the clear side cover, $2c_{si}$ for the clear spacing between the testing bar and the extended No. 8 bars, l_d for the embedment length of testing bar measured from the top surface of the UHPC strip to the end of the testing bar, and l_s for the lap splice length measured from the end of the testing bar to the end of extended No. 8 bars.

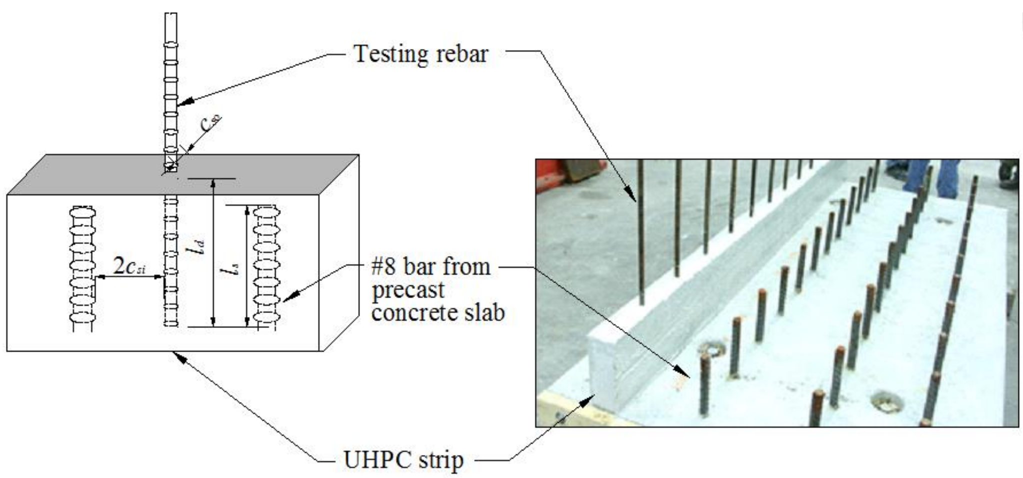

Note: c_{so}, side cover; $2c_{si}$, bar clear spacing to the adjacent No.8 bar; l_d, embedment length; l_s, lap splice length.

Figure 2. Overall configuration of test specimens.

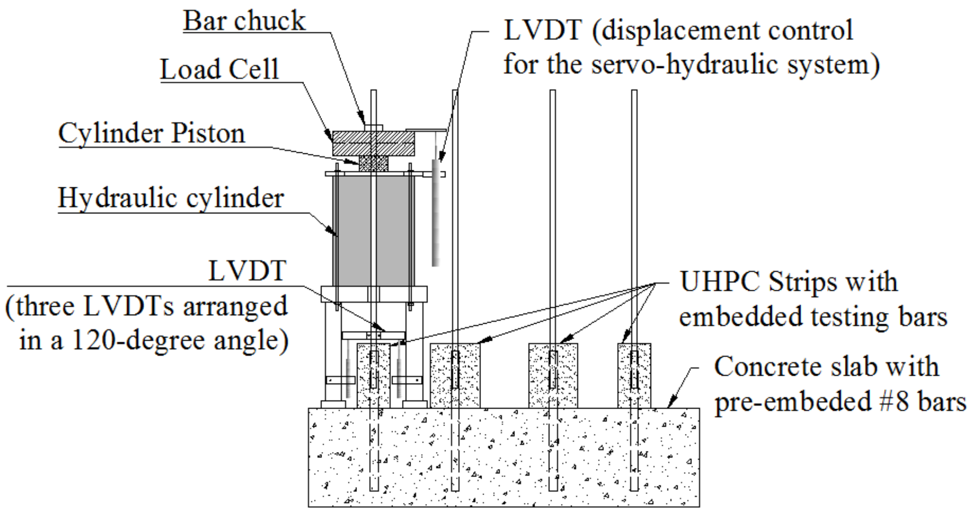

Figure 3. Loading setup.

ULTRA-HIGH PERFORMANCE CONCRETE

The results reported in this paper included three types of UHPC material, which will be reported as UHPC #1, #2, and #3. UHPC #1 is commercially available in North America, UHPC #2 is a product from Denmark, and UHPC #3 is a material developed by U.S. Army Corps of Engineers. The majority of the tests in the paper were conducted with UHPC #1, which served as the baseline for the design recommendation reported in this paper. The design recommendation was further verified with the tests with UHPC #2 and #3 and more tests with UHPC #2, #3 and other UHPC materials are being conducted. The average compressive strength at different ages for the three UHPC materials with different fiber contents are reported in Table 1. The tensile properties of these materials are also being evaluated with direct tension and splitting cylinder tests and the results are being analyzed.

Table 1. UHPC compressive strength.

	Fiber Content, by volume	Age, days	f'_c, ksi (MPa)
UHPC #1	1%	1	14 (97)
	1.5%	1	13 (90)
	2%†	1	14 (97)
		7	19 (131)
		14	21 (145)
	2.5%	1	12 (83)
	3%	1	13 (90)
UHPC #2	4.5%†	1	11 (76)
		14	19 (131)
	2%	1	9 (62)
		4	14 (97)
UHPC #3	3%†	5	15 (103)

†: Recommended fiber content by the UHPC supplier.

REINFORCING STEEL

Three types of steel bar were tested in this study, including normal strength Grade 60 uncoated and epoxy coated bars and high strength Grade 120 uncoated bars. All the Grade 60 uncoated and epoxy coated bars meet the specification of ASTM A615[14]; all the high strength Grade 120 uncoated bar meets the specification of ASTM A1035[15].

RESULTS AND DISCUSSION

A typical bar stress versus slip curve for a steel bar embedded in UHPC is presented in Figure 4. The bar stress f_s is calculated as the applied load divided by the cross section area of the bar. The displacement is measured along a loaded portion of the bar at about two inches (51 mm) above the top surface of UHPC strip. This displacement is used as a measure of the slip. The point with the maximum bar stress was marked with ($f_{s,max}$, s_1), which refers to the bar stress and slip, respectively, at bond failure. For comparison, the bar stress versus slip curve for a traditional concrete [compressive strength of 4700 psi (32.5MPa)] with the same setup as UHPC is also included in Figure 4. It should be noted that after the bar stress reaching the maximum at bond failure, the bar stress dropped quickly for the bar embedded in concrete while it gradually decreased for the bars in UHPC.

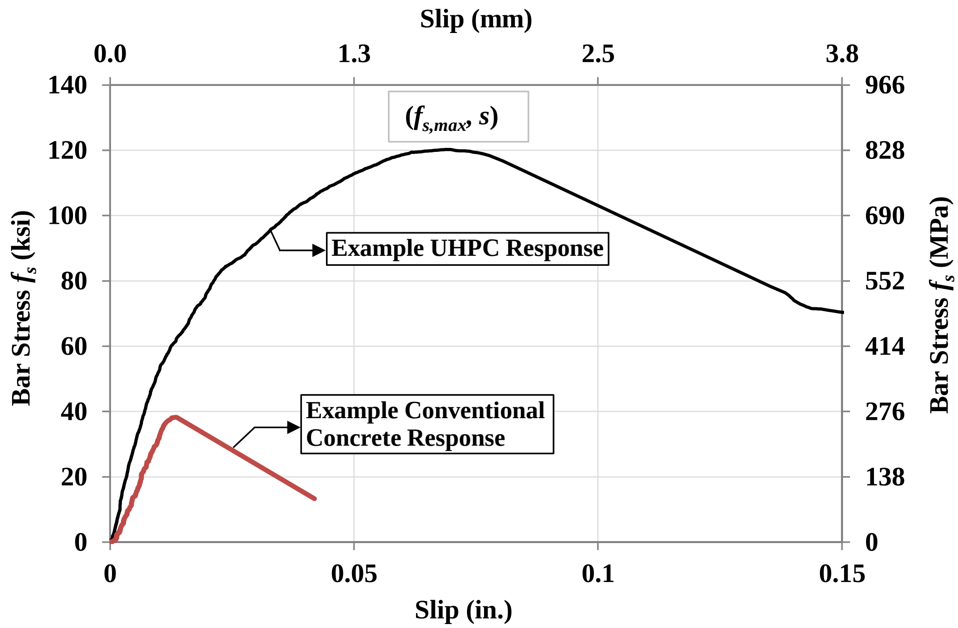

Figure 4. Bar stress versus slip at loaded bar end.

Another key term is the average bond stress at bond failure, μ_{TEST}. It is assumed that all the ribs bear against concrete and help resist the axial load at ultimate and that the bond stress distribution is uniform at the bond failure. The average bond stress can be calculated by dividing the bond force at failure by the overall contact area, using the equation in Equation 1.

$$\mu_{TEST} = \frac{f_{s,max}\pi d_b^2/4}{\pi d_b l_d} = \frac{f_{s,max} d_b}{4 l_d} \qquad \text{Eq. 1}$$

where, $f_{s,max}$ is the bar stress at bond failure, d_b is the bar diameter, and l_d is the embedment length.

CRACKING AND DAMAGE MECHANISM

In general, the transfer of force from the reinforcing steel to the surrounding concrete is mainly through mechanical anchorage or bearing of the bar ribs against the concrete corbels between ribs, with chemical adhesion and frictional forces between the bar and the concrete playing a minimal role. For the pullout tests in this study, the steel bars are lap spliced, as shown in Figure 5a, and the force on the testing bar is transferred to the concrete, which, in turn, transfers the force to the No. 8 bars that extend from the precast concrete slab. The stress distribution could cause diagonal/conical cracks due to the bearing effect and splitting cracks due to the hoop tensile stress, as shown in Figure 5b. Depending the specimens design (like embedment length, side cover, etc.) and material properties, the specimen could fail in a few different failure modes, including:

1. Diagonal/conical crack failure: the tensile forces due to the bearing effect can cause the diagonal cracks open up and thus separate a roughly planar region of concrete from the rest of the specimen.
2. Splitting crack failure: the hoop tensile stresses due to the wedging action of the deformations could split the concrete, to the side free surface and/or to the adjacent bars.
3. Pullout failure: when sufficient confinement is provided to prevent or delay the diagonal and splitting cracks, the system may fail by shearing along a surface at the top of the rib around the bars, resulting in a pullout failure.

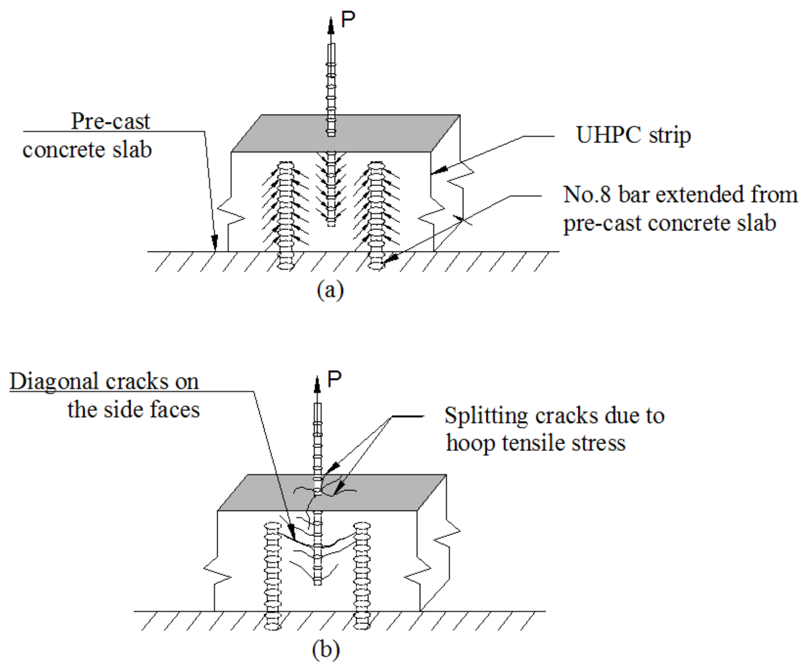

Figure 5. Pullout tests: (a) forces on bars; and (b) crack patterns.

FACTORS AFFECTING BOND

Many factors affect the bond between reinforcing bars and concrete. The factors including the embedment length, concrete side cover, bar spacing, bar size, bar type, and the UHPC material properties will be discussed in this paper.

Structural Characteristics

When the structural characteristics were evaluated, such as embedment length, side cover, and bar spacing, the tests were conducted mainly with UHPC #1 with 2% fiber by volume, which is commercially available in North America. Unless noted, all specimens were cast with the Grade 120 high strength No. 5 bars. It should also be pointed out that the majority of the tests for bar embedded in this UHPC material expressed a bond failure associated with major splitting cracks, either running to the adjacent No.8 bars, or to the side face, or both, as shown in Figure 6a. Associated with the gradual decrease on bar stress after the peak load, as shown in Figure 4, it is believed that the specimens have a pullout-like failure after reaching the peak load with the presence of splitting cracks, where are confined by fibers. In some cases, a UHPC tensile failure was observed wherein the diagonal cracks opened up and the tensile force separates a roughly planar region of concrete from the rest of the specimen, as shown in Figure 6b. In general, the specimens with UHPC tensile failures had smaller concrete side cover and shorter embedment length. More details about the failure modes can be found in the associated research report[12]. In most common conventional concrete structural applications, splitting failure is more common (ACI 408 R-03)[16].When the effect of different parameters on bond strength are evaluated, the analysis only included those with major splitting cracks.

(a)

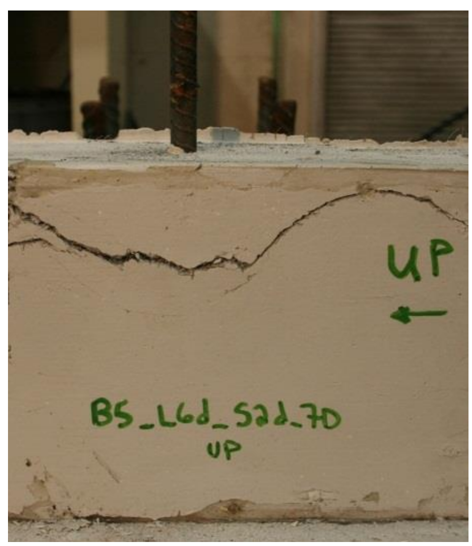

(b)

Figure 6. (a) Splitting cracks to side and adjacent bars; and (b) UHPC tensile failure with opened diagonal cracks.

Embedment Length: The bar stress at bond failure is plotted versus embedment length in Figure 7. Figure 7 includes four groups of specimens and in each group the specimens had the same design except for the embedment length. As shown in Figure 7, increasing the embedment length increases the bar stress at bond failure and the relationship between the two is nearly linear. This linear relationship observed in the study is similar to that observed in normal strength concrete (ACI 408 R-03)[16]. The linear relationship between bond force and the bonded length in normal strength concrete is often explained based on the assumption that all ribs bear against concrete at the ultimate stage and help in resisting the applied axial force, therefore at ultimate the bond stress distribution is nearly uniform. However, the bond stress distribution in high strength concrete, with compressive strength over 13 ksi (90 MPa) and without fiber reinforcement, was found to be not uniform based on a study conducted by Azizinamini et al.[17] Azizinamini et al. noted that for high strength concrete, the increase in bearing capacity is more than the increase in tensile strength, which in turn, would prevent crushing of the concrete in the vicinity of each rib to the extent that would otherwise take place in normal strength concrete. In other words, the high strength concrete would crack before crushing the concrete in the vicinity of each rib. All ribs may not participate in resisting applied axial load before the concrete cracks, and the first few ribs contribute the most. The observed linear relationship between bond strength and embedment length implies that the behavior attributed to traditional high strength concretes by Azizinamini et al. [17] may not be present in UHPC, potentially due to the enhanced pre- and post-cracking tensile response of the UHPC.

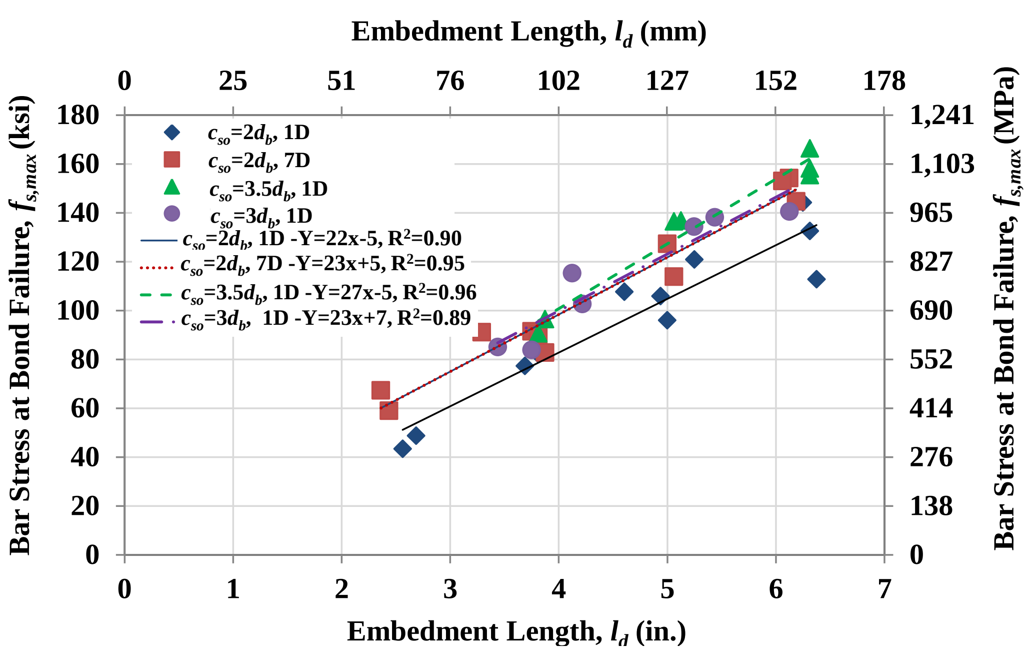

Note: c_{so} represents the side cover, d_b represents the bar diameter, and D represents the testing age in days.

Figure 7. Effect of embedment length: $f_{s,max}$ versus embedment length l_d.

Side Cover: The side cover is normally paired with bar spacing, which together provide the confinement for the embedded bar. In general, for bond failure involving splitting of the concrete, the nature of the splitting failure depends on whether the concrete cover, $c_{so,}$ is smaller than c_{si}, which is half of the clear spacing to adjacent bar. When c_{so} is smaller than c_{si}, the splitting crack occurs through the side cover to the free surface. When c_{si} is smaller than c_{so}, the splitting crack forms between the reinforcing bars. The results for the effect of the side cover are presented in Figure 8. The specimens in the figure are grouped based on embedment length and within each group, the specimens have the same design except for side cover. The bond strength, μ_{TEST}, is used here, where the embedment length was included in the calculation. In this way, all specimens in the figure can be compared equally as a whole. As shown, the bond strength increased as the side cover increased. When half of the bar clear spacing (c_{si}) is smaller than the side cover (c_{so}), the bond strength still increases as the side cover (c_{so}) increases, instead of being controlled by half of the bar clear spacing (c_{si}). The bond strength seemed to flatten out when the side cover is greater than the clear spacing $2c_{si}$. It should be noted that for the specimens having side cover values close to their bar spacing, the side cover is big enough that the specimens failed at bar stresses near to the ultimate bar strength for the bar used in this study.

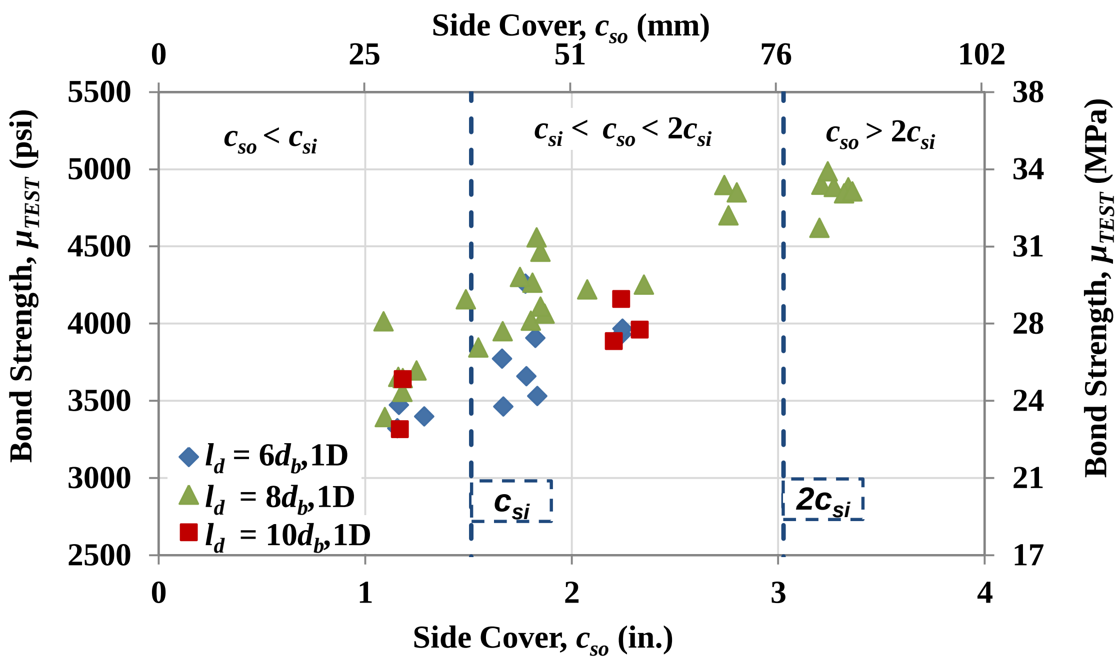

Note: l_d represents embedment length, d_b represents the bar diameter, and D represent the testing age in days. All specimens were designed to have the same bar spacing (c_{si}) and UHPC compressive strength.

Figure 8. Effect of side cover: bond strength μ_{TEST} versus side cover.

<u>*Bar Spacing:*</u> As stated earlier, bar spacing is generally paired with concrete side cover. Besides the side cover, two other cases are also considered here: zero bar spacing with contact lap slice and far away bar spacing with values greater than $l_s tan(\theta)$. The geometrical demonstration of $l_s tan(\theta)$ is shown in Figure 9a. The consideration here is that the bond strength for contact lap splice specimens can be affected due to decreased contact area between the steel bar and UHPC materials, especially considering the dispersion of the fiber reinforcement. When the adjacent bars are placed far away, greater than $l_s tan(\theta)$, the adjacent

bars would not help to stop the propagation of the diagonal cracks and the bond strength would likely to be primarily dependent on the tensile mechanical performance of the UHPC.

A few observations were made when the effect of bar spacing is investigated. For the non-contact lap spliced specimens with bar spacing less than $l_s tan(\theta)$, no obvious correlation between bond strength and bar spacing is noted. The specimens were divided into three groups based on bar spacing, including those with zero spacing, those with far away spacing having values greater than $l_s tan(\theta)$, and those with the bar spacing between contact and $l_s tan(\theta)$, as shown in Figure 9b, c, and d. The $2d_b$ spacing is the minimum spacing, other than contact lap splice, tested in the study. As shown, the average bond strength reduced slightly when the bars are in contact versus those spaced between $2d_b$ and $l_s tan(\theta)$; for the specimens with far away bar spacing, they also had a reduction on the bond strength.

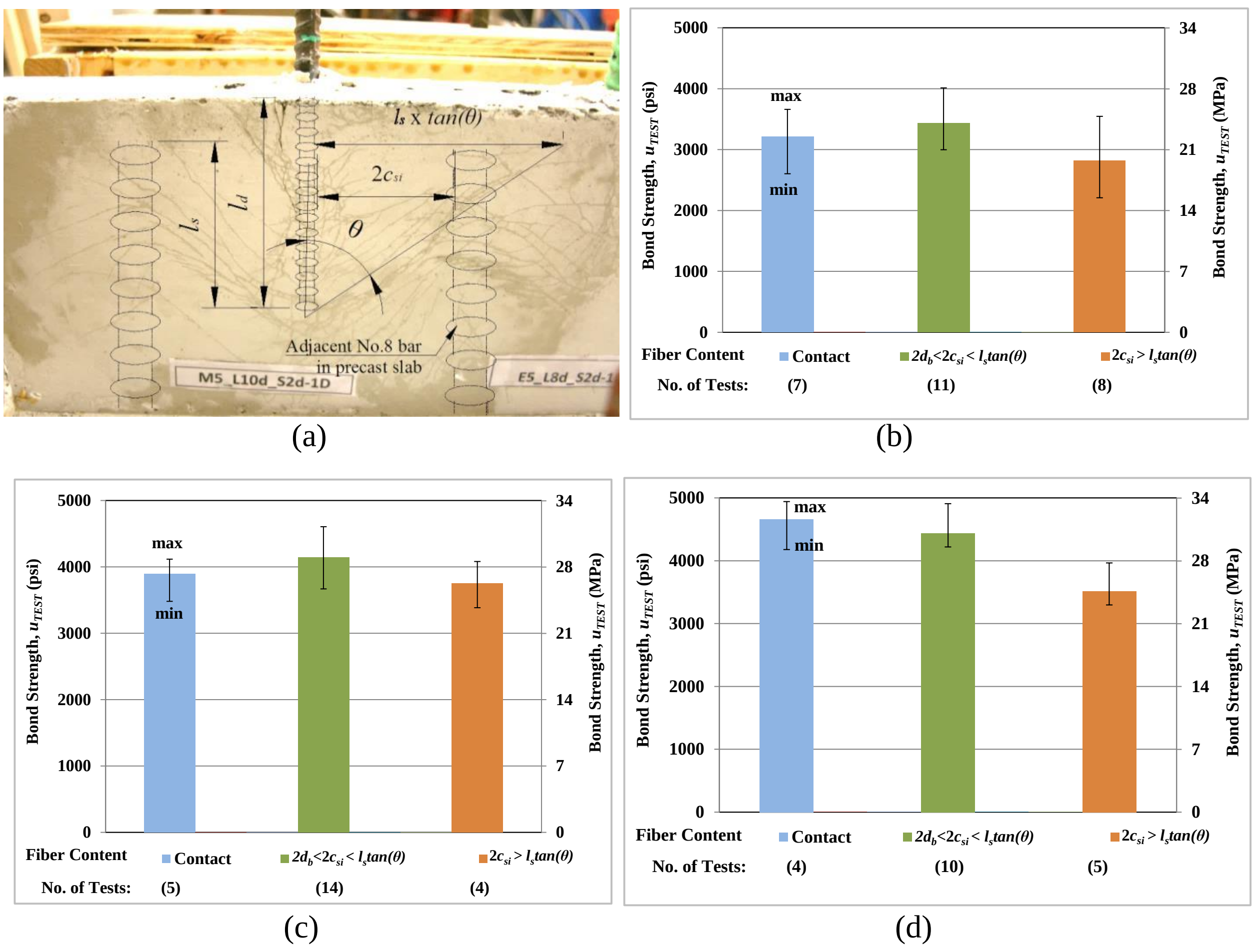

Figure 9. (a) Geometrical demonstration of $l_s tan(\theta)$ and $2c_{si}$; Effect of bar spacing: bond strength μ_{TEST} versus $2c_{si}$ for specimens with: (b) embedment length $8d_b$, side cover $2d_b$; (c) embedment length $8d_b$, side cover $3d_b$; and (d) embedment length $8d_b$, side cover $3.5d_b$.

Minimum Bar Stress of Lesser of Yield or 75 ksi (517 Mpa)

One of the main goals of the research is to develop design recommendations for steel reinforcing bars embedded in UHPC. The fundamental design concept embedded into the reinforcing steel development and splice length provisions of the AASHTO LRFD Bridge Design Specification and the ACI 318 Building Code is to allow for the attainment of the yield strength of the mild steel reinforcement. The research studies on which these provisions are based were primarily conducted on structural components wherein the stress in the reinforcement at failure was below the yield stress of the bar. These results allowed for extrapolation of the observed bar stress at failure up to the yield strength of the bar. Aside from special provisions that ensure ductility by limiting the locations of splices or anchorages, these design specifications do not specifically ensure ductility of spliced or embedded reinforcing bars beyond the initial yielding of the bar. Accordingly, the results obtained in this study were analyzed so as to create design guidance that parallels the existing provisions in these design specifications. Specifically, test results were analyzed to ensure that the bar could attain the lesser of its yield stress or 75 ksi (517 MPa).

The bar stress at bond failure is plotted versus embedment length in Figure 10a for all the high strength No. 5 bars tested in study. The specimens had a variety of side cover and bar spacing. For the side cover, values of $2d_b$, $2.7d_b$, $3d_b$,and $3.5d_b$ were included; for the bar spacing to the nearest No. 8 bars, values of 0, 2, 4, 6, 8, and 12 in. (0, 51, 102, 152, 203 and 305 mm) were used. It should be noted that the specimens with conical UHPC tensile failure and the specimens close the casting point, which tend to having lower bond strength than those failed with splitting cracks and those cast distance away from the casting point[12], are all included in the figure. The specimens were grouped into two base categories, one with side over equal to $2d_b$ and the other one with side cover greater than or equal to $2.7d_b$, as shown in Figure 10a. Then, the specimens with those specific conditions, including the zero bar spacing, bar spacing greater than $l_s tan(\theta)$, end specimens close to casting point, and specimens with UHPC tensile failures were marked on top of the base categories, as explained in the note of Figure 10. For those without any mark on top, they all had bar spacing between $2d_b$ and $l_s tan(\theta)$. It is also important to note that all the tests included were conducted at one day after casting with a UHPC compressive strength of approximately 13.5 ksi (93.1 MPa).

As shown in Figure 10a, the large majority of the specimens had a bar stress at bond failure over 80 ksi (552 MPa); the ones with bar stress at bond failure below 80 ksi (552 MPa) were those with a side cover of $2d_b$, combined with either a short embedment length of $4d_b$ and $6d_b$ or disadvantageous spacing (bar spacing = 0 or bar spacing > $l_s tan(\theta)$). It is also important to note that for the specimens with a side cover of $2d_b$, combined with sufficient embedment length ($\geq 8d_b$) and appropriate bar spacing (between $2d_b$ and $l_s tan(\theta)$ in this study), they all have reached a bar stress of at least 80 ksi (552 MPa). Figure 10b only include those specimens with side covers greater than $2d_b$. As shown, all specimens exhibited a bar stress higher than 80 ksi (552 MPa), with the specimens with bar spacing equal to zero or greater than $l_s tan(\theta)$ and/or end specimens close to casting point generally exhibiting lesser bar stresses at bond failure. It should be noted that there is only one specimen that failed with UHPC tensile failure in this group. The specimens with an embedment length of $8d_b$ and a

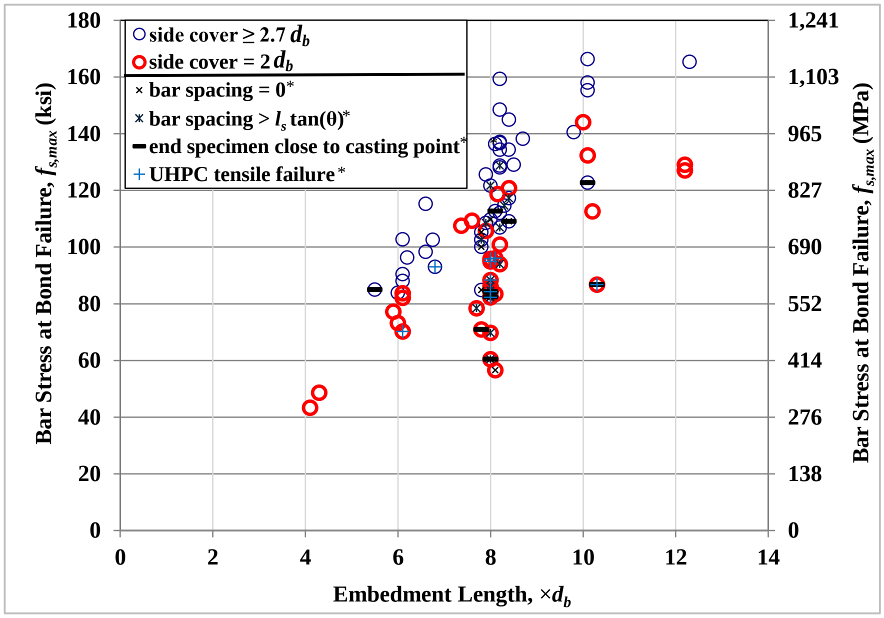

(a)

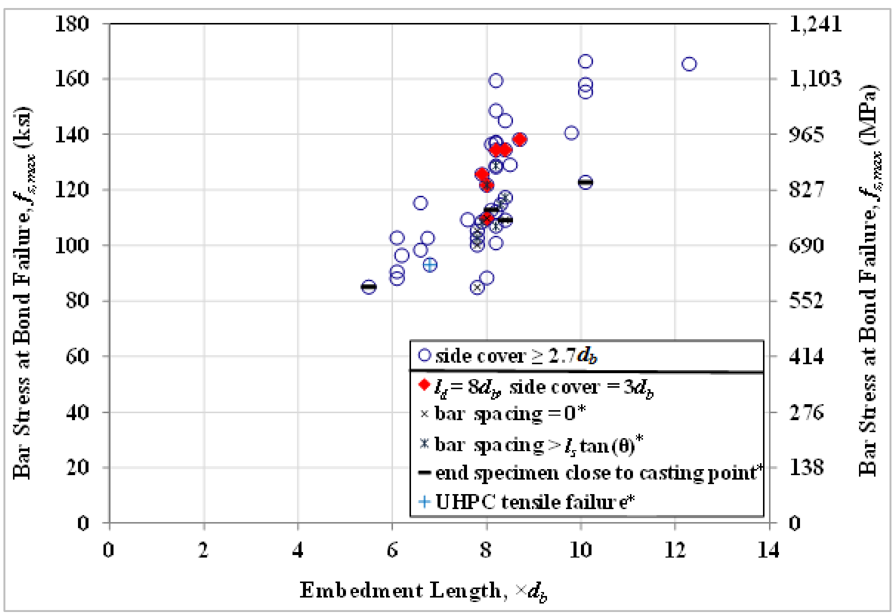

(b)

Note: * Specimens were grouped into two base categories based in side cover, one with side cover equal to 2d_b and the other one with side cover greater than or equal to 2.7d_b. The specimens with specific conditions, including bar spacing equal to zero, bar spacing greater than $l_s tan(\theta)$, end specimens close to casting point, and specimens with UHPC tensile failures were marked on top of that. For example, refers to a specimen with side cover of 2d_b and with a specific condition of end specimen close to the casting point; refers to a specimen with side cover ≥ 2.7d_b, and with specific conditions of zero bar spacing to nearest bar and end specimen close to the casting point. For those without any mark on top, they had bar spacing between 2d_b and $l_s tan(\theta)$.

Figure 10. Graph. Bar stress at bond failure versus embedment length for (a) all tests with A1035 No. 5 bars; and (b) all tests with A1035 bars and with a side cover ≥ 2.7d_b.

side cover of $3d_b$ are identified in Figure 10b with a red diamond; all of them have reached a bar stress over 100 ksi (690 MPa) at bond failure; those with preferred bar spacing [between $2d_b$ and $l_s tan(\theta)$] reached a bar stress over 120 ksi (827 MPa).

With the results presented in Figure 10 and considerations for practical construction and safety margins, a design with a minimum embedment length of $8d_b$, a minimum side cover of $3d_b$, a bar clear spacing between $2d_b$ and l_s, and a minimum UHPC compressive strength of 13.5 ksi (93.1 MPa) is recommended. When different bar type (ASTM A615 Grade 60 epoxy coated and uncoated bars and ASTM A1035 Grade 120 uncoated bars) and bar size (from No. 4 to No.11) are considered, the research by Yuan and Graybeal[12,13] found that for bars with larger diameter, the bond strength decreased, but not in a significant manner; bars that yield before bond failure exhibit less ultimate pull-out load than geometrically similar high yield strength bars subjected to the same loading conditions. The design stated above with an embedment length of $8d_b$ and a side cover of $3d_b$ would reach at least of lesser of the bar yield stress or 75 ksi (517 MPa) at bond failure for all the bar types and sizes tested in the study. For example, for Grade 60 epoxy coated and uncoated No. 5 bars, they had a bar stress at bond failure of 81 and 96 ksi (558 and 662 MPA), respectively, for a design with an embedment length of $8d_b$ and side cover of only $2d_b$. For the Grade 120 No. 11 bars tested, they had a bar stress at bond failure of 76 ksi (524 MPa) with an embedment length of $6d_b$ and side cover of $2d_b$. Therefore, it would be conservative to expect bar stress at bond failure to be at least the lesser of 75 ksi (517 MPa) or the bar yield strength with an embedment length of $8d_b$ and side cover of $3d_b$.

Material Properties

Compressive Strength and Fiber Contents: Traditionally, the effect of concrete properties on bond strength is represented by the square root of the compressive strength, which is related to the tensile strength of the concrete. The bond strength μ_{TEST} is plotted versus $f'_c{}^{1/2}$ in Figure 11. All the specimens in Figure 11 were cast with UHPC #1 with a fiber content of 2% and designed to have the same side cover of 1.25 in. (32 mm) and bar center spacing of 4 in. (102 mm). As expected, an increase in the compressive strength increases the bond strength, but the correlation coefficient (R^2) values are low. Since the UHPC material investigated is both high strength and fiber reinforced, other material properties besides compressive strength such as tensile strength and fracture energy should be involved in the evaluating of bond strength.

The point that other material properties besides compressive strength are needed to characterize this type of material is further reinforced when the effect of fiber content is investigated. Figure 12 presents the bond strength versus the fiber content. All the specimens in Figure 12 were cast with UHPC #1 material with various fiber contents and they all had the design that was recommended in previous section, which had a side cover $3d_b$ and embedment length of $8d_b$. As shown in Figure 12, when the fiber content increased from 1% to 2% by volume, the bond strength was greatly increased; however, the compressive strength of these materials with different fiber contents were every similar, as shown in Table 1, about 13 or 14 ksi (90 or 97 MPa). When the fiber content was increased to 3%, the bond strength was about the same as those with 2% fiber. It was noted that the specimens with 2.5% fiber had a lower bond strength than those with 2 and 3%, which is probably due to fiber segregation as indicated with high dynamic flow. The fiber segregation will be discussed in later section. These results demonstrated that the fiber content does have effect on the bond strength. In general, more fibers will lead to higher bond strength, but not necessarily compressive strength; when the fiber content is higher than certain threshold, the further contribution of the fibers to the bond strength is limited. Other material properties, including the tensile strength, fracture energy, and toughness are being evaluated for this type of materials and the results will be reported in the future.

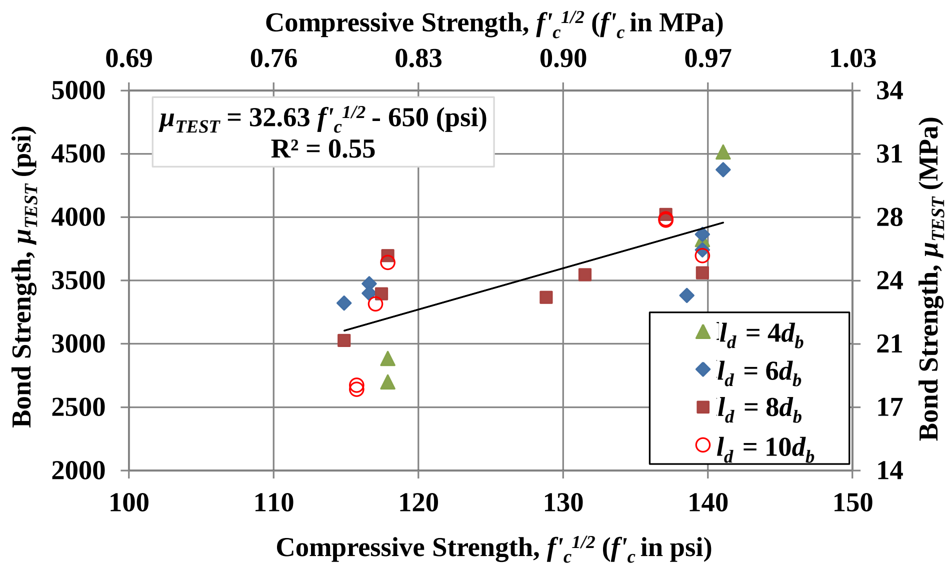

Note: All specimens had the same side cover and bar spacing.

Figure 11 Effect of compressive strength: u_{TEST} versus $f'_c{}^{1/2}$

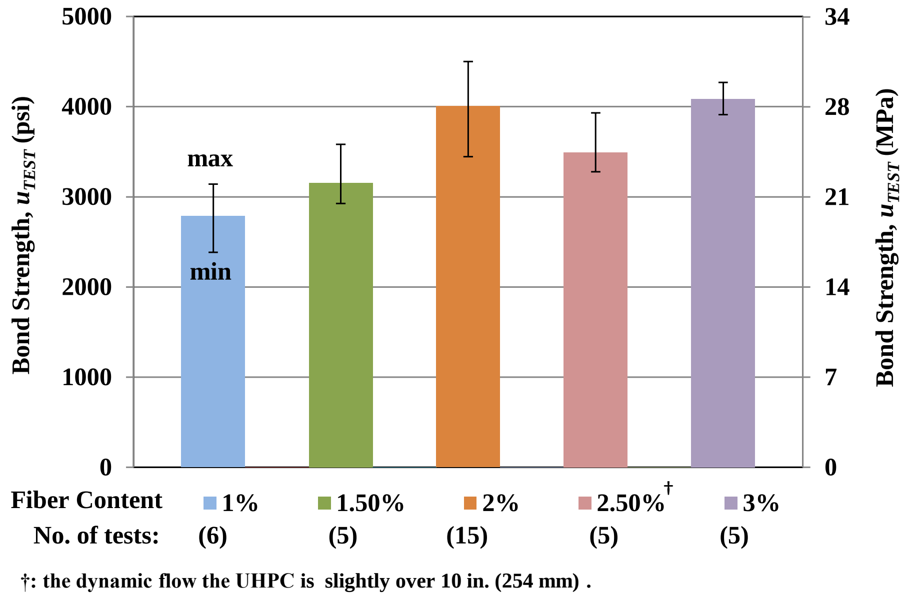

†: the dynamic flow the UHPC is slightly over 10 in. (254 mm) .

Figure 12 Effect of fiber content: u_{TEST} versus fiber content (by volume)

It should also be noted that when the fiber contents changed, the failure mode also changed at bond failure. As mentioned earlier, when the structural characteristics were evaluated using UHPC #1 with a fiber content of 2%, most specimens failed with the presence of opened splitting cracks, as shown in Figure 6a. When the fiber content was reduced to 1%, it was found that the majority of the specimens failed with opened diagonal cracks, as shown in Figure 13a. When the fiber content increased to 1.5%, the specimens tended to fail with opened splitting cracks and the splitting cracks were wider than those observed with specimens having more fibers.

(a) (b)

Figure 13. (a) UHPC #1 with 1% fiber, by volume; (b) UHPC #1 with 1.5% fiber, by volume.

Fiber Distribution: The fiber orientation and distribution are always concerns for fiber reinforced concrete. In this study, the UHPC #1, independent of the fiber content up to 3%, is flowable enough that during casting the material was first poured in from one end and allowed to flow until the forms were mostly filled. Thereafter, the UHPC was poured in from the middle locations[12,13]. A demonstration of the form setup and material casting are presented in Figure 14 a and b. For UHPC materials that are not very flowable, like UHPC #2 in this study, they were poured along the strip and vibrated after casting (as recommended by the UHPC supplier). Pictures of UHPC #2 casting and vibrating are presented in Figure 14 c and d. One way to measure the flowability is to conduct ASTM C 1437[18] flow tests, which is adopted and modified in this study. The modification is to have 20 drops instead of 25 drops for the dynamic flow measurements. A demonstration of the UHPC flow after 20 drops for UHPC #1 and #2 are shown in Figure 15 a and b, respectively.

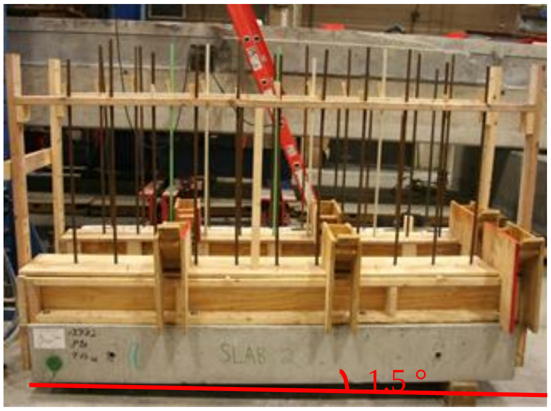

(a) (b)

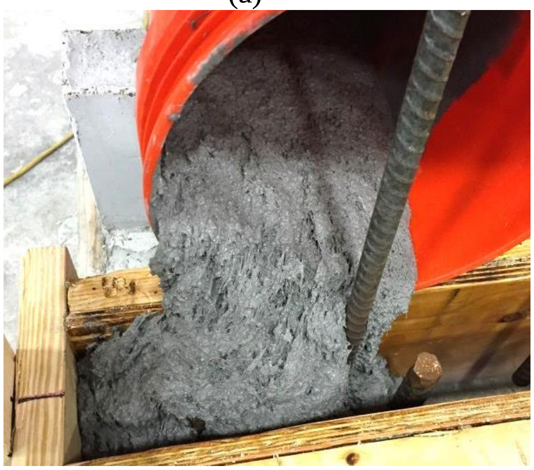

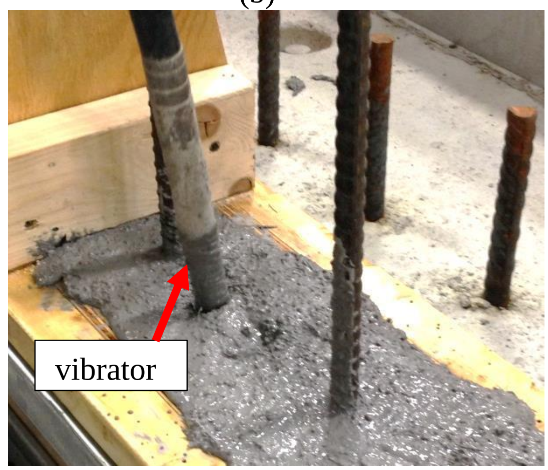

(c) (d)

Figure 14 (a) UHPC #1, casting form setup; (b) UHPC #1, casting from one end; (c) UHPC #2 casting; and (d) UHPC #2 vibrating.

(a) (b)

Figure 15 ASTM C1437 flow tests after 20 drops: (a) UHPC #1; (b) UHPC #2.

For UHPC materials like UHPC #2 tested in the study, it took more effort for construction as the material itself did not flow, which may limit its deployment in certain applications. For materials like UHPC #1, it is relatively easier for construction due to its flowability. However, cautions should be given when using a material like UHPC #1 as fiber segregation could occur when it is very flowable. The results from current study show that when the dynamic flow after 20 drop was over 10 in. (254 mm), fiber segregation was observed, which can lead to lower bond strength. Figure 16 shows the specimens with the exact same design, but one set with very flowable material having over 10 in. (254 mm) flow and one set with flowable material but less than 10 in. (254 mm) flow. As shown, the very flowable material had a significant bond strength reduction, which is likely due to fiber segregation. As current practice, a dynamic flow value of less than 10 in. (254 mm) after 20 drops is recommended. More tests are being conducted in an effort to identify the fiber segregation in hardened UHPC.

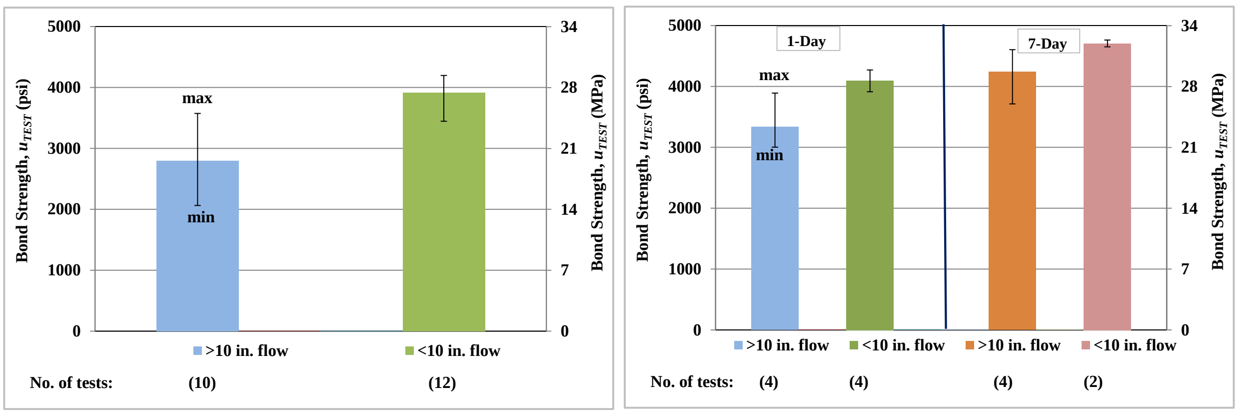

(a) (b)

Figure 16. Bond strength versus flowability: (a) UHPC #1 with 2% fiber; (b) UHPC #1 with 3% fiber.

CONCLUSIONS

The bond strength of mild steel reinforcing bars in UHPC was evaluated in this study. It was found that the bond behavior of deformed bar in UHPC is different from that in traditional concrete in many aspects. The following conclusions were developed based on the results of the tests completed in the study.

- Increasing the embedment length of the steel bar increases the ultimate pull-out force at bond failure; a linear relationship between the pull-out force and the bonded length is observed.
- Bond strength increases as the side cover increases.
- When the bar spacing is too close that limits the ability of the fiber reinforcement to locally enhance the mechanical resistance of the UHPC, or the bar spacing is too large that the induced diagonal cracks from the pullout force will not intersect with the adjacent bars, the specimens have lower bond strength than those with bar spacing

between the two conditions; when the bar spacing is between the two conditions, it does not seem to have much effect on the bond strength.

- An increase in the compressive strength of the UHPC results in an increased bond strength. However, the effect of UHPC properties on bond strength cannot be effectively represented solely by the compressive strength.
- The fiber content has effect on the bond strength. In general, more fibers lead to higher bond strength, but not necessarily compressive strength; when the fiber content is higher than certain threshold, the further contribution of the fibers to the bond strength is limited.
- Fiber segregation in very flowable UHPC materials can cause a decrease on the bond strength.

RECOMMENDED DESIGN

One of the main goals of the research is to develop design recommendations for steel bar embedded in UHPC, thus providing guidance for designers using reinforced UHPC in innovative applications. Deformed reinforcing bar embedded in UHPC can attain the lesser of the bar yield strength or 75 ksi (517 MPa) at bond failure when the following conditions are met:

- Bar size from No. 4 to No. 11,
- Uncoated or epoxy coated bar,
- Minimum embedment length of $8d_b$,
- Minimum side cover of $3d_b$,
- Bar clear spacing between $2d_b$ and l_s,
- Minimum UHPC compressive strength of 13.5 ksi (93 MPa), and
- A maximum flow of 10 in. (254 mm) after 20 drops following the ASTM C1437 tests was recommended to minimize fiber segregation.

For lap splice reinforcement configurations, a minimum lap splice length of 75 percent of the embedment length is suggested, which is the range into which most of tests in this study fell. Note that d_b is the bar diameter and l_s is the lap splice length.

For situations wherein the above conditions are met except that the minimum side cover is between $2d_b$ and $3d_b$, the minimum embedment length should be increased to $10d_b$.

Refinements of the recommended design can be made for specific applications. For example, if a larger side cover is provided, and/or UHPC has gained higher compressive strength, an embedment length reduction may be possible. The supporting information can be found in the associated research report. [12]

Note that the above design recommendation is based on the one UHPC material that is widely available in North America. The recommended design is further evaluated with UHPC materials from other suppliers. The preliminary results are presented in Table 2. All the specimens in Table 2 used the recommended mix design and fiber content by the suppliers, except for UHPC #2 with 2% fiber, where the supplier recommended content is 4.5%. They were all tested with No. 5 bars and designed to have an embedment length of $8d_b$, a side cover of $3d_b$, and a bar center to center spacing of 4 in. (102mm) (clear spacing between $2d_b$ and l_s). As shown, they all reached a bar stress at bond failure well above 75 ksi (517 MPa).

Table 2. Bar stress at bond failure for different UHPC formulas

		UHPC #1	**UHPC #2**		**UHPC #3**
Fiber content, by volume		2%	4.5%	2%	3%
f', ksi (MPa)		13.5 (93)	10.8 (74)	13.6 (94)	15.2 (105)
ASTM C1437 Flow Test (20 drops), in. (mm)		9.2 (234)	5.6 (143)	7.5 (191)	8 (203)
$f_{s,\,max}$ at bond failure, ksi (MPa)	average	132 (909)	147 (1015)	126 (866)	125 (862)
	minimum	117 (806)	131 (906)	118 (811)	123 (848)
	maximum	143 (985)	157 (1086)	135 (928)	130 (896)
No. of Tests		10	6	4	3

As a continuing effort, other material properties, such as the tensile strength, fracture energy, and toughness, are being evaluated and a general expression to estimate the bond strength of deformed steel bar in UHPC materials is being developed.

ACKNOWLEDGEMENTS

The research project discussed herein could not have been completed were it not for the dedicated support of the federal and contract staff associated with the FHWA Structural Concrete Research Program. Recognition goes to William Lee, Tim Tuggle, Andrei Denes, and Kevin Deasy, all technicians in the FHWA Structural Testing Laboratory, for their assistance in completing the experimental testing program. The publication of this manuscript does not necessarily indicate approval or endorsement of the findings, opinions, conclusions, or recommendations either inferred or specifically expressed herein by the Federal Highway Administration or the United States Government.

REFERENCES

1. Graybeal, B., “Ultra-High Performance Concrete,” U.S. Department of Transportation, Federal Highway Administration, FHWA-HRT-11-038, 2011, 8 pp.
2. Graybeal, B., “Material Property Characterization of Ultra-High Performance Concrete,” Federal Highway Administration, Report No. FHWA-HRT-06-103, 2006, 186 pp.
3. Graybeal, B., “Behavior of Field-Cast Ultra-High Performance Concrete Bridge Deck Connections Under Cyclic and Static Structural Loading,” Report No. PB2011-101995, National Technical Information Service, Springfield, VA, 2010.

4. Graybeal, B., "Development of a Field-Cast Ultra-High Performance Concrete Composite Connection Detail for Precast Concrete Bridge Decks," Report No. PB2012-107569, National Technical Information Service, Springfield, VA, 2012.
5. Yuan, J. and Graybeal, B., "Adjacent Box Beam Connections," *Proc., PCI National Bridge Conference,* Washington, D.C, 2014.
6. Yuan, J. and Graybeal, B., "Full-Scale Testing Of Shear Key Designs For Box-Beam Bridges," ASCE Bridge Journal, 2015, in review.
7. Ultra-High Performance Concrete, U.S. Department of Transportation, Federal Highway Administration. *https://www.fhwa.dot.gov/research/resources/uhpc/.*
8. Fehling, E., Lorenz, P., and Leutbecher, T., "Experimental Investigations on Anchorage of Rebars in UHPC," *Proceedings of Hipermat 2012 3rd International Symposium on UHPC and Nanotechnology for High Performance Construction Materials,* University Press, Kassel, Germany, 2012, pp. 533–540.
9. Swenty, M. and Graybeal, B., "Influence of Differential Deflection on Staged Construction Deck-Level Connections," FHWA, U.S. Department of Transportation, Report No. FHWAHRT-12-057, National Technical Information Service Accession No. PB2012-111528, 2012.
10.Holschemacher, K., Weiβe, D., and Klotz, S., "Bond of Reinforcement in Ultra High Strength Concrete," *Proceedings of the International Symposium on Ultra High Performance Concrete*, University Press, Kassel, Germany, 2004, pp. 375–387.
11. Holschemacher, K., Weiße, D., and Klotz, S., "Bond of Reinforcement in Ultra High-Strength Concrete," *Seventh International Symposium on the Utilization of High-Strength/High-Performance Concrete*, Vol. I, Publication No. SP-228, Ed., Russell, H.G., American Concrete Institute, Farmington Hills, MI, 2005, pp. 513–528.
12. Yuan, J and Graybeal, B., "Bond Behavior of Reinforcing Steel in Ultra-High Performance Concrete," FHWA-HRT-14-090, Department of Transportation, Federal Highway Administration, VA, 2014.
13. Yuan, J. and Graybeal, B. (in press), "Bond Of Reinforcement In Ultra-High Performance Concrete," ACI Structural journal, 2015.
14. ASTM A615/A615M-13, "Standard Specification for Deformed and Plain Carbon-Steel Bars for Concrete Reinforcement," *ASTM Book of Standards Volume 01.04,* ASTM International, West Conshohocken, PA, 2013.
15. ASTM A1035/A1035M-13b, "Standard Specification for Deformed and Plain, Low-Carbon, Chromium, Steel Bars for Concrete Reinforcement," *ASTM Book of Standards Volume 01.04,* ASTM International, West Conshohocken, PA, 2013.
16. ACI Committee 408, Bond and Development of Reinforcement, *Bond and Development of Straight Reinforcing Bars in Tension* (ACI 408R-03), American Concrete Institute, Farmington Hills, MI, 2003, 49 pp.
17. Azizinamini, A., Stark, M., Toller, J.J., and Ghosh, S.K., "Bond Performance of Reinforcing Bars Embedded in High-Strength Concrete," *ACI Structural Journal*, V. 90, No. 5, Sep.-Nov., 1993, pp. 554-561.
18. ASTM C1437-13, "Standard Specification for Flow of Hydraulic Cement Mortar," *ASTM Book of Standards Volume 04.01*, ASTM International, West Conshohocken, PA, 2013.